The activation energies of crystallization in the amorphous alloy METGLAS® 2826A

M. VON HEIMENDAHL, G. KUGLSTATTER*
Institut für Werkstoffwissenschaften I, Universität Erlangen-Nürnberg, Martensstraße 5, D-8520 Erlangen, W. Germany

Nucleation and growth rates of the MSI metastable phase crystals of the amorphous alloy $Fe_{32}Ni_{36}Cr_{14}P_{12}B_6$ have been studied in detail using quantitative transmission electron microscopy. Three different types of activation energies are involved in the crystallization: E_n for nucleation, E_g for growth of the crystals, and E_c for the whole process of crystallization. All three were determined experimentally: E_n and E_g in the present paper and E_c in a former work. A general formula was developed which combines the three and was found to be in good agreement with the experimental values. Furthermore, attention has been drawn to the experimental value of the Avrami exponent which is in very good agreement with a detailed theory developed in 1955 by Ilschner, and differing with common literature values. Also, the diffusivity of metalloid in this alloy has been reported using the growth rate of MSI crystals.

1. Introduction

In an earlier paper [1] we emphasized that different activation energies should be distinguished in a crystallization process. These are: (i) that for nucleation of crystals, called E_n in this paper, (ii) that for growth of crystals, E_g, and finally (iii) that for the whole process of crystallization, E_c. The latter combines (i) and (ii) by referring to the kinetics of the total volume fraction of all the crystals. All three may be determined independently by experiment: (i) by counting crystal numbers in the transmission electron microscope (TEM), (ii) by measuring their size in the TEM and (iii) either by quantitative TEM or, better, by integrating methods such as differential thermal analysis/differential scanning calorimetry (DTA/DSC), dilatometry (length effects), etc. The values given in [1] were only preliminary and in the meantime more detailed work has been carried out in order to answer most of the questions left open in [1].

A theoretical connection is expected to exist between E_n, E_g and E_c. Recently, formulae to correlate these three activation energies have been developed by Ranganathan and Heimendahl [2]. The application of these formulae to the case of

2826A and comparison with the present experimental data is also reported in this paper. Finally, the kinetic data obtained for 2826A are compared with the values obtained from a theory given by Ilschner a long time ago [3] which he developed for the analogous case of diffusion-controlled growth of precipitates. Also, the growth rate of the metastable phase MSI has been used to evaluate the diffusivity of metalloid in this alloy.

2. Experimental and methodical techniques

As the question of the reproducibility of the results of [1] has been often raised and discussed [4] a separate series of experiments were carried out on samples produced by the same technique [1]. For this purpose, samples were chosen from two different batches with a gap of three years, called Series I and III, respectively, in this paper. The material was Metglas® 2826A as in [1], made by Allied Chemical Corp., USA. Furthermore, to check possible variations within one ribbon, a Sample II was analysed; this was taken from the same ribbon as Series I but from a spot a distance of 8 m from where Sample I was taken. Concerning annealing and TEM specimen preparation, the
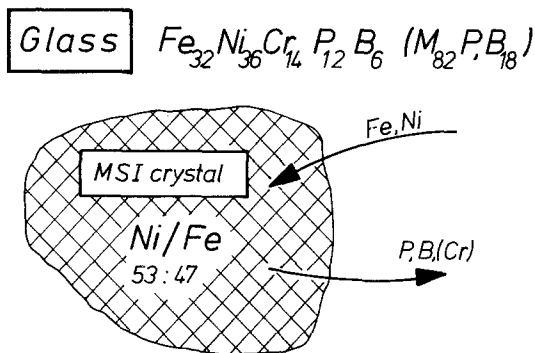
---

*Present address: KWU Erlangen, W. Germany.

Figure 1 Schematic drawing illustrating the atomic movements involved in the crystallization of the MSI phase in the alloy 2826A, according to [6].

same methods were applied as in [1]. Since the kinetics of crystallization is strongly dependent upon temperature, a careful temperature control of $\pm 1°$ C was maintained in the salt bath.

It was assumed that each nucleus results in one crystal, i.e. in counting the number of nuclei, the crystals were counted. To obtain the crystal density, $n(t, T)$, (at time t and temperature T) the foil thickness of the TEM samples was determined by the latex ball method [5]. Of course, there is a lower limit of instrumental resolution below which a crystal can no longer be seen. In the present case this was at a diameter of about 6 nm. (The finite foil thickness of 30 to 80 nm makes contrast of smaller crystals too poor.) For determining E_n, this "cutting effect" in counting $n(t, T)$ is negligible.

To measure the size of the crystals, the diameter s of the largest crystal was taken. It is assumed that smaller crystals were the result of later nucleation, i.e. ones which started to grow after the incubation period. Thus, from $s(t)$ the apparent diffusion coefficient D can be calculated from

$$s/2 = A (Dt)^{1/2} \qquad (1)$$

for the case of parabolic growth. In our case, D refers to the diffusion of the elements Fe and Ni into the MSI crystals (Fig. 1) and the metalloids P and B outwards, i.e. into the glass. (These compositional changes were proven by Heimendahl and Oppolzer [6].) Since the partial diffusivities of the individual elements at present cannot be distinguished by these experiments, Equation 1 deals with the apparent diffusion coefficient.

Strictly, A is not a constant but is slightly tem-perature-dependent because it contains the equilibrium solubilities at the glass–crystal phase boundaries. However, in our case the crystallization occurs in the lower portion of the time–temperature–transformation (TTT)-diagram (in the temperature range below the "nose" of this diagram). Therefore, any change in the above-mentioned solubilities is negligibly small in the present, narrow temperature range of crystallization (350 to 375° C) which lies much below the melting temperature according to the relevant phase diagram. Thus, A can be approximately taken as constant in this case. (See Section 4.4 also.)

If the crystal density becomes too large, the pictures blur due to crystal overlap. Therefore, only the initial part of the crystallization was analysed in the following plots (only up to 10% total volume fraction, which corresponds approximately to 30% of the attainable MSI phase). This paper deals exclusively with the first crystallization stage, called MSI; the other stages are dealt with in [1].

In the case of clustered crystals, forming an image similar to a cauliflower or a blackberry, it was attempted to count and to measure the individual crystals, although this was sometimes difficult.

If the nucleation rate $\dot{n}$ is constant for each individual temperature T, $\dot{n}$ can be written as

$$\dot{n} = \text{constant} \cdot \exp{(-E_n/RT)}, \qquad (2)$$

where E_n is the apparent activation energy of nucleation and R is the gas constant. Equation 2 is an approximation valid for small volume fractions of crystals. As mentioned above, for other reasons analysis was in any case carried out only for small volume fractions of less than 10%. It is not the purpose of this paper to discuss generally the constituent parts contributing to E_n. However, it may be mentioned that in the present case of a long range diffusion*-controlled, classical homogeneous nucleation, $E_n = E_g + \Delta G_c$, (Equation 49.2 in [7]) where ΔG_c is the thermodynamic work barrier for the formation of the critical nucleus and E_g is the activation energy of growth. E_g is equal to E_d the activation energy of (long-range) diffusion, if growth is diffusion-controlled (parabolic). Again, as explained above for A, the slight changes of ΔG_c within the temperature range observed in our experiments are negligible.

---

*Concerning the terms long-range and small-range diffusion; by mistake in our earlier paper the MSI reaction was called "small-range diffusion-controlled" instead of long-range.
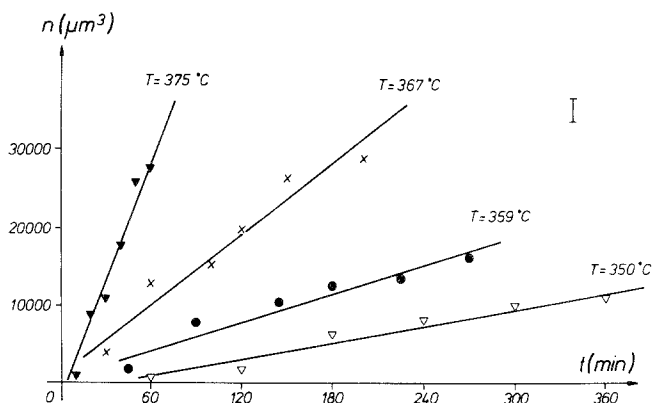
$n \, (\mu m^3)$

Figure 2 Number of crystals in the amorphous alloy METGLAS® 2826A after isothermal annealings at 4 different temperatures.

From the linear plots of $s^2(t)$ for each temperature T, the diffusion constant $D(T)$ was obtained from Equation 1 and, of course,

$$D = \text{constant} \cdot \exp\left(-E_g/RT\right) \qquad (3)$$

in our case.

3. Results

The plots of Figs 2 and 3 show $n(t)$ and $s^2(t)$ for the four temperatures chosen; 350, 359, 367 and 375° C. These temperatures were selected because at lower temperatures the reaction goes exceedingly slowly, and at higher temperatures too quickly (see also the TTT-diagram of Fig. 11 in [8]). One notices that in this temperature range $\dot{n}$ is approximately constant, which indicates homogeneous, steady-state nucleation. In a recent review Köster and Herold [9] deal with different types of nucleation kinetics, e.g. "quenched-in nuclei", "transient nucleation" and "steady-state nucleation". Obviously, only the latter occurs if the presuppositions used for MSI in 2826A described in this paper are valid, i.e. constant nucleation rate.

Of course there is inevitably a certain amount of scatter for each measured point. The indicated error bar is the mean value of all the standard error bars of the individual measured points. The latter are the results of three to five TEM enlargements magnified typically 180 000 times for analysis, each giving one value. Fig. 4 is a typical TEM bright-field image. (For details of the relevant microstructures in this alloy, see [1, 10].) One cannot expect a precise value with this sort of statistical measurement, but it turns out, that for the present purpose, i.e. determining activation energies; the procedure is satisfactory. The Arrhenius plots in Figs 5 and 6 show that fairly good straight lines can be drawn through the points, each representing the slope of one of the lines in Figs 2 and 3. The prefactor A in Equation 1 was taken as unity in this case. (For determination of E_g from Equation 3 the value of A is immaterial if it is constant over the temperature
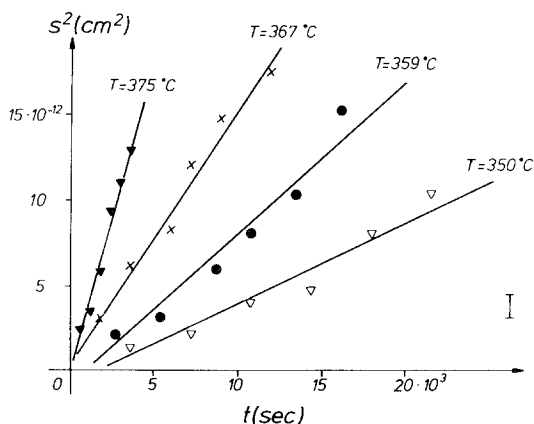

Figure 3 Maximum diameters of crystals (squared) after the same thermal treatments as given in Fig. 2.
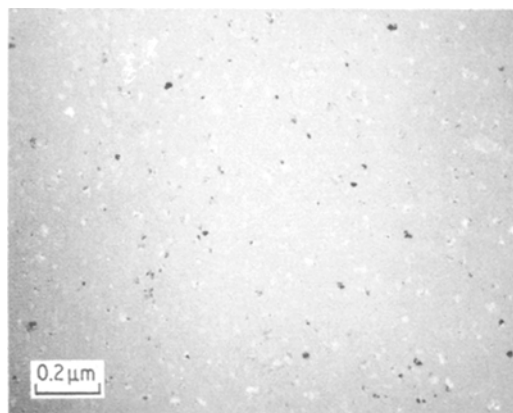

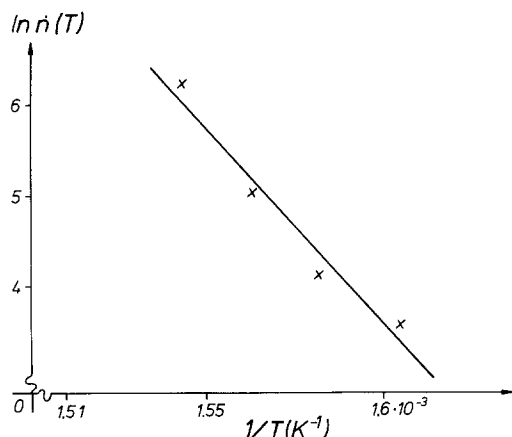*Figure 4* Typical transmission electron micrograph of the MSI-phase crystals, 4 h, 350° C.

Figure 5 Arrhenius plot obtained from the data of Fig. 2 for determination of the activation energy of nucleation, E_n, after Equation 2.
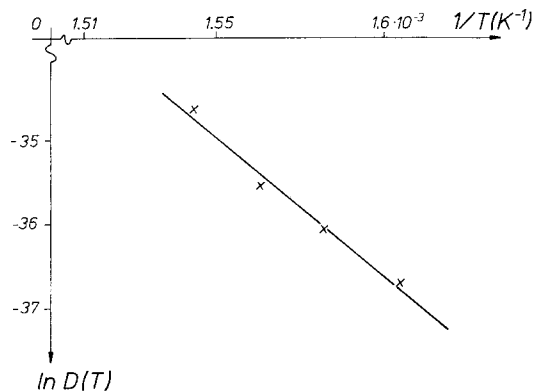

Figure 6 Arrenhius plot for the diffusion coefficient $D(T)$, which was obtained from Fig. 3. From the slope of this figure, the activation energy E_g follows. D in cm^2 sec^{-1}.

range.) From the slope of Figs 5 and 6 again, by means of Equations 2 and 3, we obtain the activation energies listed in Table IA and B. Considering the different error sources involved, we estimate the average accuracy to be ± 10% of the given values.

4. Discussion
4.1. Reproducibility from batch to batch
The results for the apparent activation energies show that the reproducibility is fairly good from batch to batch (Series I compared with Series III) and within one batch (Sample I compared with Sample II) as well. In Series I a second analysis was performed from the same samples. Scatter of the results seems to be less for E_n than for E_g, but this may be due to the inherent inaccuracy involved in the measurement of s. This result may not be generally true, of course. In other metallic glass materials or with other production techniques, there may occur certain variations in crystallization behaviour and kinetics from batch to batch, but at least in the present case, of 2826A, the results

TABLE IA Activation energies in Metglas® 2826A, MSI – crystallization

	E_n (nucleation) (kJ mol^{-1})	E_g (growth) (kJ mol^{-1})
Series I	359	272
Series I (2nd analysis)	–	236
Series II	345	229
Series III	358	271
Mean value	354	252

were consistent within the limits of accuracy as described.

4.2. Comparison of E_n and E_g with E_c from the formula and experiments
The following formula, recently developed [2], combines the quantities described and defined in the introduction

$$E_c = \frac{a E_n + bp E_g}{a + bp}, \tag{4}$$

where $p = 1$ for linear growth, $p = 1/2$ for parabolic growth, $b = 1$, 2 or 3 for one- two- or three-dimensional growth, $a = 0$ for no nucleation (i.e. zero nucleation rate, all nuclei being frozen in at the beginning), $a = 1$ for a constant nucleation rate, $0 < a < 1$ for a decreasing nucleation rate and $a > 1$ for an increasing nucleation rate. (a also may be expressed as in the form $n = n_0 t^a$, n is the number of nuclei and n_0 is a constant [14]).

Thus, Equation 4 gives E_c as a weighted mean of E_n and E_g including the coefficients cited. The basis for the derivation of Equation 4 in [2] is the classical Johnson–Mehl–Avrami kinetic approach, refined by putting in the activation energies for nucleation, growth and the whole process. Although much work has been done in terms of the

TABLE IB

	E_c (total process)
By experiment [1]	270
By experiment [11]	286
By formula, with E_n and E_g	293

theory of related reaction kinetics, by Christian [7], to our knowledge no formula such as Equation 4, combining all the different cases which are possible, has been published before. Taking mean values from Table I of $E_n = 354 \, \text{kJ mol}^{-1}$, $E_g = 252 \, \text{kJ mol}^{-1}$ and $p = 1/2$, $b = 3$ and $a = 1$ (the constant nucleation rate is proved by Fig. 1), it follows that $E_c = 293 \, \text{kJ mol}^{-1}$. This is not far from the experimentally observed value of $E_c = 270 \, \text{kJ mol}^{-1}$ obtained by quantitative metallography (TEM volume fraction) in [10] (see also Table I in [1]) and agrees very well with the value $E_c = 286 \, \text{kJ mol}^{-1}$ reported by Antonione et al. [11], using differential thermal analysis, which is also an integrating technique. Thus, we may conclude that at least in the present case Equation 4 is in good agreement with two different experimental results. Another case of successful application of Equation 4 is reported by Ranganathan et al. [8] and Tiwari et al. [12] concerning $Fe_{40}Ni_{40}P_{14}B_6$ (Metglas 2826A). More work needs to be done to check Equation 4 with other alloys and this is in progress. Relatively few studies have been published so far regarding the experimental determination of nucleation and growth, e.g. [13], measuring them separately.

4.3. Kinetics and especially the Avrami exponent

Figs 2 and 3 show that, owing to scatter of experimental points, an incubation time in 2826A cannot reliably be detected in the temperature range used. At first sight, this could seem contradictory to Fig. 7 in [10], where the plot of volume fraction of MSI at 350° C starts only after 2 h. However, in Fig. 7 of [10] no values smaller than 1% could be plotted owing to graphical limitations. On the other hand, one can calculate that the volume fraction from the data of Figs 2 and 3 for 350° C below 2 h is less than 1%, e.g. after 1 h only about 0.05%. In this context, the difficulty of determining the incubation times in general should be stressed; our example shows how it depends on sensitivity of detecting or plotting the real beginning of crystallization.

Another important aspect of kinetics is the Avrami exponent, m, in the equation for transformed volume fraction, $x(t)$,

$$x(t) = 1 - \exp{(-t/\tau)^m}, \qquad (5)$$

where τ is the time constant. m was reported to be 1.7 in our earlier work [1] and was obtained by TEM quantitative analysis. This value is in excellent agreement with the theoretical value of $m = 5/3 \approx 1.7$ predicted many years ago by Ilschner [3]. His theory deals with the completely analogous case of precipitation from crystalline solid solutions, governed by nucleation and long-range diffusion-controlled growth (parabolic growth).* It modifies the Avrami kinetic by careful mathematical treatment of the diffusion equations. The theory also distinguishes the cases $a = 0$ (no nucleation) and $a = 1$ (constant nucleation rate) for which m is $1 < m < 1.2$ and $m = 1.7$, respectively. We would like to point out that Ilschner [3] seems somehow to be overlooked in the literature. Rather, even comprehensive monographs such as by Christian [7] printed many years later, still report m values following $m = a + pb$ (the same notation as above), e.g. p. 542 in Christian's book [7]. For our case m would be $1 + 3/2 = 2.5$, which is not in accordance with either the theoretical [3] value or our own experimental work above ($m = 1.7$). (Also, the formula $m = 5/2 + a$, used by Boswell [14] and taken from Burke [15], seems to be doubtful in this light.) The more precise m-values from [3] should generally be used.

4.4. Absolute diffusion values

Recently, Köster and Herold [16] reported the absolute diffusion data for Fe—Ni—B metallic glasses based on the same method as here, i.e. size measurement and application of Equation 1. For primary reaction types and in the vicinity of 360° C their Fig. 1 yields values between 10^{-18} and $10^{-19} \, \text{m}^2 \, \text{sec}^{-1}$. To determine D from Equation 1, the value of A is needed. A closely consideration, using thermodynamic and alloy data for our case [17], yielded $A = 1.1$. Using this, the diffusion coefficient D comes out 15 times smaller than that reported by Köster and Herold [16]. We think that this may be due to the fact that the phosphorus contained in 2826A may slow down the diffusion. However, further systematic investigations are recommended in this direction.

---

*It was shown earlier [6] that MSI is a "primary" crystallization and therefore the same physical conditions are involved as in a diffusion-controlled, homogeneous precipitation from crystalline solid solutions. Concerning the term "primary", see [4, 9].

4.5. Non-uniformity of specimens

Leake and Greer [18] also report on investigations about the "non-uniformity of specimens" with regard to the determination of E_c (in $Fe_{80}B_{20}$). In addition, they consider critically some other interesting potential influences on E_c. These concern: temperature lag between sample and sample holder or furnace in the DSC/DTA, changes in the homogeneous amorphous structure prior to or during crystallization, and the validity of the Arrhenius approximation. (Is there only *one* E_c, and is it constant? It *is* only one, if T_c, the temperature of crystallization, is far below the nose of the relevant TTT-diagram, which is the case for the measurements on 2826A reported in this paper.)

Acknowledgements

References

1. M. von HEIMENDAHL and G. MAUSSNER, *J. Mater. Sci.* **14** (1979) 1238.
2. S. RANGANATHAN and M. von HEIMENDAHL, *ibid.* (in press).
3. B. ILSCHNER, *Archiv f.d. Eissenhüttenwesen* **26** (1955) 59.
4. U. KÖSTER and U. HEROLD, Proceedings of the 3rd International Conference on Rapidly Quenched Metals, Brighton, 1978 (The Metals Society, London, 1978).
5. M. von HEIMENDAHL, *Micron* **4** (1973) 111.
6. M. von HEIMENDAHL and H. OPPOLZER, *Scripta Met.* **12** (1978) 1087.
7. J. W. CHRISTIAN, "The Theory of Transformation in Metals and Alloys", Part I, 2nd edn, (Pergamon Press, Oxford, 1975) pp. 437–41.
8. S. RANGANATHAN, J.-C. CLAUS, R. S. TIWARI and M. von HEIMENDAHL, Conference on Metallic Glasses, Budapest, June/July, 1980.
9. U. KÖSTER and U. HEROLD, in "Glassy Metals I", edited by H. J. Güntherodt, (Springer Verlag, Berlin, 1981).
10. M. von HEIMENDAHL and G. MAUSSNER, Proceedings of the 3rd International Conference on Rapidly Quenched Metals, Brighton, 1978, Vol. I, (The Metals Society, London, 1978) p. 424.
11. C. ANTONIONE, L. BATTEZZATI, A. LUCCI, R. RIONTINO and G. VENTURELLO, *Scripta Met.* **12** (1978) 1011.
12. R. S. TIWARI, S. RANGANATHAN and M. von HEIMENDAHL, to be published.
13. U. KÖSTER, U. HEROLD, F. NOLTE and H. WEISSENBERG, Conference on Metallic Glasses, Budapest, June/July, 1980.
14. P. G. BOSWELL, *J. Mater. Sci.* **15** (1980) 1939.
15. J. BURKE, "The Kinetics of Phase Transformations" (Pergamon Press, Oxford, 1965).
16. U. KÖSTER and U. HEROLD, *J. de Physique*, Colloque C-8 **41** (1980) 352.
17. J. WILDE, unpublished work (1980).
18. J. A. LEAKE and A. L. GREER, *J. Non-Cryst. Sol.* **38/39** (1980) 735.